Plate impulse response spatial interpolation with sub-Nyquist sampling

G. Chardon[a], A. Leblanc[b], L. Daudet[a,c]

[a] *Institut Langevin - Ondes et Images, ESPCI, CNRS UMR 7587*
10 rue Vauquelin F-75231 Paris Cedex 05 France
[b] *Univ Lille Nord de France, F-59000 Lille, France*
UArtois, LGCgE, F-62400 Béthune, France
[c] *Paris Diderot University and Institut Universitaire de France*

Abstract

Impulse responses of vibrating plates are classically measured on a fine spatial grid satisfying the Shannon-Nyquist spatial sampling criterion, and interpolated between measurement points. For homogeneous and isotropic plates, this study proposed a more efficient sampling and interpolation process, inspired by the recent paradigm of compressed sensing. Remarkably, this method can accomodate any star-convex shape and unspecified boundary conditions. Here, impulse responses are first decomposed as sums of damped sinusoids, using the Simultaneous Orthogonal Matching Pursuit algorithm. Finally, modes are interpolated using a plane wave decomposition. As a beneficial side effect, these algorithms can also be used to obtain the dispersion curve of the plate with a limited number of measurements. Experimental results are given for 3 different plates of different shapes and boundary conditions, and compared to classical Shannon interpolation.

Keywords: plate vibration, compressed sensing, impulse response interpolation, plane wave approximation

Email addresses: gilles.chardon@espci.fr (G. Chardon), alexandre.leblanc@univ-artois.fr (A. Leblanc), laurent.daudet@espci.fr (L. Daudet)

1. Introduction

For a wide variety of engineering applications, plate characterization requires its full set of impulse responses (IRs). In structural health monitoring (SHM) for example, IRs are needed to obtain the free response of the inspected structure [1]. Furthermore, combining this set of IRs together with cross correlation techniques has been successfully used for SHM purposes [2], or impact localization [3], leading to the realization of tactile-acoustical interfaces.

For all the above-mentioned applications, existing IR methods rely on a comprehensive knowledge of the object under study. In order to know the IR at any position on the plate, the following procedure is usually carried out : IRs are measured on a fine spatial sampling grid, and interpolation schemes are used to estimate the IRs between sampling points. While both computational power and data storage capabilities continue to increase, the acquisition of the IRs on a very fine grid can still be a daunting task. When acquisition time is limited, synthesizing large IR data-sets from as few measurements as possible, can a highly relevant problem.

Classical schemes for determination of plate IRs can be classified in two categories:

- experimental methods, with various excitation types (impulses, chirps, harmonic excitations, etc.) where the IRs are sampled on a grid with a spatial step given by the Shannon-Nyquist sampling criterion;
- numerical methods, aiming at the resolution of the equations governing the movement of the plate, such as classical Finite Element Methods [4], or methods using particular properties of the solutions of the Helmholtz equation, such as the Ultra Weak Variational Formulation [5], the Variational Theory of Complex Rays [6] or the Non-dimensional Dynamic Influence Function method, using plane waves [7] or Bessel functions [8].

Both types of methods have drawbacks: experimental methods need a high number of measurements, especially at high frequencies, and numerical methods

need a detailed knowledge of the plate : mechanical properties of the materials, boundary conditions, etc.

Here, we propose a new IR determination scheme for homogeneous, isotropic plates *of any star-convex shape and arbitrary boundary conditions*. This new method is an hybrid between experimental and numerical methods and thus can be interpreted in two different ways:

- as an experimental method, this method allows the reduction of the number of measurements below the number required by the sampling theorem, and where IRs are interpolated using simple physical knowledge (the Kirchoff thin-plate model under isotropy and homogeneity assumptions)
- or, alternatively, as a numerical method, the knowledge of the material and the boundary conditions is no longer required thanks to a few experimental measurements.

The method is based on the classical Kirchhoff thin-plate model with a simple damping model. In that case, a approximation of the bending modes is performed using a sparse set of plane waves. Therefore, we can use the recent paradigm of so-called compressed sensing [9]: if a signal is known to be sparse in a given basis, it can be recovered using much less samples than the full set of regular samples required by the Shannon sampling theorem. Particularly, sparse trigonometrical polynomials (i.e., sparse sums of plane waves in two dimensions), can be recovered from randomly placed local measurements [10] [11]. Moreover, in our case, the sparsity is structured, in the sense that the planes waves used in the sum share the same wave number. An algorithm specially designed for the recovery of such signals is introduced, yielding accurate reconstructions of the modal shapes with sub-Nyquist sampling, even when the sampling pattern is regular, at the cost of a small error .

Similar ideas were introduced in [12], where room impulse responses are interpolated and extrapolated with few measurements. It was, however, limited to parallelepipedic rooms and along a line parallel to a wall, while the method presented in this paper works with arbitrary shapes and in two dimensions.

The proposed interpolation scheme is confirmed experimentally with IR measurements on plates with various shapes. One significant feature of the method is to achieve a full characterization of its impulse responses is achieved with significantly less measurements than required by the Nyquist spatial sampling rate.

This paper explores the different trade-offs and strategies for spatially sampling the IRs, and verifies the relevance of this approach on experimental data. As a beneficial side effect, the proposed algorithm can also be used to painlessly characterize the dispersion curve of the media, in the full bandwidth under study (here in the audio range 0 - 22 kHz), using a reduced set of IR measurements, independently of the boundary conditions.

The following section introduces the physical model of the plate used in the subsequent developments. The Simultaneous Orthogonal Matching Pursuit (SOMP) and its use for the mode identification is described in section 3, and the interpolation algorithm is introduced in Section 4. Finally, experimental results are discussed in the last section before the conclusion of the paper.

2. Physical model

Assuming Kirchhoff-Love hypothesis and a simple damping model, the transverse displacement $w(x, y, t)$ of a homogeneous and isotropic thin plate obeys the equation

$$\rho h \frac{\partial^2 w}{\partial t^2} + \alpha \frac{\partial w}{\partial t} + D\Delta^2 w = 0$$

and appropriate boundary conditions. Here ρ is the density, h the thickness, $D = Eh^3/12(1-\nu^2)$ the bending stiffness, (E the Young's modulus, and μ the Poisson ration).

With w_n the modes of the bilaplacian Δ^2 and k_n^4 the related eigenvalues, the displacement can be decomposed as

$$w(x, y, t) = \sum_{n \in \mathbf{N}} q_n(t) w_n(x, y)$$

As the modes are linearly independent, each q_n obeys the equation

$$\rho h \frac{\partial^2 q_n}{\partial t^2} + \alpha \frac{\partial q_n}{\partial t} + D k_n^4 q_n = 0$$

The solutions of these equations are damped sinusoids, and the displacement writes

$$w(x,y,t) = \sum_{n \in \mathbf{N}} A_n e^{-a_n t} \cos(\omega_n t + \phi_n) w_n(x,y)$$

The modes w_n can be decomposed as a sum of two solutions of the Helmholtz equation w_n^+ and w_n^- [13]:

$$\Delta w_n^+ - k_n^2 w_n^+ = 0, \quad \Delta w_n^- + k_n^2 w_n^- = 0$$

If the plate is star-shaped, the w_n^- can be well approximated [14] [15] by a finite sum of M propagative plane waves $u^-_{\vec{k}_{n,m}}(\vec{r}) = e^{i(\vec{k}_{n,m} \cdot \vec{x})}$, with $||\vec{k}_{n,m}|| = k_n = \omega_n / c$

$$w_n^-(x,y) \simeq \sum_{m=1}^{M} w_{nm} u^-_{\vec{k}_{n,m}}(x,y)$$

With similar arguments, the w_n^+ can be approximated by sum of M functions $u^+_{\vec{k}_{n,m}}(\vec{r}) = e^{(\vec{k}_{n,m} \cdot \vec{x})}$ which will be called *exponential plane waves* in the remainder of the paper.

Finally, as the bandwidth of the measured impulse responses is finite, only a finite number N of modes are observed, and the displacement can be approximated by the sum

$$w(x,y,t) \simeq \sum_{n=0}^{N} A_n e^{-a_n t} \cos(\omega_n t + \phi_n) \left(\sum_{m=1}^{M} w^-_{nm} e^{i \vec{k}_{nm} \cdot \vec{x}} + \sum_{m=1}^{M} w^+_{nm} e^{\vec{k}_{nm} \cdot \vec{x}} \right)$$

Using this model, impulse response can be interpolated from a small set of samples with these successive steps, outlined in figure 1 :

- modal frequencies and dampings of the modes are extracted, and used to determine the amplitudes and phases of the modal shapes at the measurement points. This is detailed in section 3.
- the undersampled modal shapes are interpolated by computing the coefficients w^-_{nm} and w^+_{nm}, as discussed in section 4.

- the interpolated modal shapes and the identified sinusoids are then simply recombined to compute the interpolated impulse responses.

This model is similar to the model used in the Method of Fundamental Solutions [16, 17, 18] : the part of the modal shape expressed as a sum of secodn kind Hankel functions $H_0^2(k|x|)$ is here approximated by a sum of propagative waves, while the part expressed as a sum of first kind Hankel functions with imaginary argument $H_0^1(ik|x|)$ is written as a sum of exponential waves. An advantage of the plane wave model over the MFS model is that it does not need the choice of source points, as a set of plane waves with regular angular space works for any star-convex shape.

3. Mode identification

The first step is to identify the frequencies and dampings associated to each mode. For this task the Simultaneous Orthogonal Matching Pursuit (SOMP) [19] algorithm is used.

SOMP belongs to the class of sparse approximation algorithms, that aim at decomposing signals as combinations of few elementary functions chosen from a redundant dictionary, here damped sinusoids of the form $c_{a,\omega,\phi}(t) = e^{-at}\cos(\omega t + \phi)$ [20].

For instance, greedy algorithms, such as the widely-used Matching Pursuit [21], identify these atoms one by one, as follows :

1. find the atom (here, the damped sinusoid $c_{a,\omega,\phi}$) most correlated with the signal,
2. subtract its contribution from the signals
3. repeat until halting conditions are met

In our case, the SOMP algorithm goes as follows : step (1) is achieved by computing the scalar products between the signal and all candidate damped sinusoids $c_{a,\omega}$ with various damping a, and frequencies ω (typically on a uniform grid). For increased robustness, this frequency analysis is performed over all

measured IRs simultaneously, and therefore the criteria for choosing the best matching damped sinusoid is to maximize the sum, over all channels (measured IRs), of the scalar products between a candidate damped sinusoids and the signals at the m-th iteration:

$$C_m(a, \omega, \phi) = \sum_k | \langle \hat{c}_{a,\omega,\phi}, u_{k,m} \rangle |^2$$

where $\hat{c}_{a,\omega,\phi}$ are damped sinusoids normalized such that $||\hat{c}_{a,\omega,\phi}|| = 1$, and $u_{k,m}$ is the signal of the channel k at the m-th iteration.

At step (2), we subtract the orthogonal projection of the signals onto the subspace spanned by the set of damped sinusoids already identified:

$$u_{k,m+1} = u_{k,m} - P_m(u_{k,m})$$

where P_m is the orthogonal projection on the space spanned by the identified sinusoids, implemented iteratively via QR factorization for efficiency.

It should be noted that, instead of computing correlations for different phases, this algorithm computes the norm of the orthogonal projection onto the space spanned by the complex sinusoid of a given frequency and damping and its conjugate, $\tilde{c}_{a,\omega,\phi}(t) = e^{(i\omega - a)t}$ and $\tilde{c}^{\star}_{a,\omega,\phi}(t) = e^{(-i\omega - a)t}$. With this method, there is no need to test sinusoids with various phases, avoiding the discretization of the phases and accelerating the computation. The norm of the projection can be easily computed using the scalar products with the complex damped sinusoids, themselves computed using the Fast Fourier transform algorithm, thanks to the equality :

$$\sum_n s_n(e^{(-i\nu - \alpha)n}) = \sum_n (s_n e^{-\alpha n}) e^{-i\nu n}$$

The algorithm is stopped when a predefined number of sinusoids are identified, or when the energy of the residual drops below a predefined threshold.

Using multiple channels simultaneously has significant advantages. Identifying the modes on a single channel would fail when the measurement point lies on a nodal line of one of the modes. Furthermore, the fusion of modal parameters

estimates obtained for each channel is not a straightforward task. Finally, a channel-by-channel implementation would be slower, as QR factorizations have to be computed separately for each channel, whereas only one is needed for the multichannel implementation.

Other algorithms can be used for this task, such as high resolution algorithms like MUSIC or ESPRIT [22], using the specific properties of the damped sinusoids. However, they have little interest for the problem at hand. Their main advantage is their high resolution, but, in our case, two modes too close to be separated with Fourier-based algorithms have similar wavenumber and the sum of these modes, while not being a mode itself, will still be well approximated by a sparse sum of plane waves.

4. Mode interpolation

Once the modes are identified, a plane wave approximation of each mode is performed. As only a small number of plane waves are needed, this decomposition is based on a small number of parameters - it can thus be expected that these can be estimated using only a low number of measurements (e.g. less than required by the Nyquist spatial sampling criterion)

In this approximation and for a given mode, the key point is that all plane waves that form this linear decomposition have the same (unknown) modulus, i.e. the wavenumber k. In other words, a mode with wavenumber k_0 belongs to the subspace $\mathcal{E}_{k_0}$ spanned by the set of plane waves with wave vectors $k_0\vec{u}_\theta$, where $\vec{u}_\theta$ is the vector of norm 1 of orientation θ.

Thus, k_0 can be found by searching amongst all candidate subspaces $\mathcal{E}_k$, the one that minimizes the distance between itself and the mode considered or, equivalently, that maximizes the norm of the orthogonal projection of the mode on $\mathcal{E}_k$.

In practical implementations, two discretizations will be used : the modes will be spatially sampled on a finite number n_m of points p_j, and the subspace $\mathcal{E}_k$ will be approximated by the subspace E_k spanned by a finite number n_w of

plane waves, themselves sampled at the points p_j, with vectors u_m uniformly distributed along the unit circle (figure 2). With $\mathbf{W}_k$ the matrix containing the plane waves in E_k :

$$\mathbf{W}_k = \begin{pmatrix} e^{ik\vec{u}_1\cdot\vec{x}_1} & \dots & e^{ik\vec{u}_M\cdot\vec{x}_1} & e^{k\vec{u}_1\cdot\vec{x}_1} & \dots & e^{k\vec{u}_M\cdot\vec{x}_1} \\ \vdots & & \vdots & \vdots & & \vdots \\ e^{ik\vec{u}_1\cdot\vec{x}_j} & \ddots & e^{ik\vec{u}_M\cdot\vec{x}_j} & e^{k\vec{u}_1\cdot\vec{x}_j} & \ddots & e^{k\vec{u}_M\cdot\vec{x}_j} \\ \vdots & & \vdots & \vdots & & \vdots \\ e^{ik\vec{u}_1\cdot\vec{x}_J} & \dots & e^{ik\vec{u}_M\cdot\vec{x}_J} & e^{k\vec{u}_1\cdot\vec{x}_J} & \dots & e^{k\vec{u}_M\cdot\vec{x}_J} \end{pmatrix}$$

the projector on E_k writes $\mathbf{P}_k = \mathbf{W}_k\mathbf{W}_k^\dagger$, † denoting the Moore-Penrose pseudo-inverse. The estimation $\hat{k}$ of the wave number is given by

$$\hat{k} = \text{argmax}_k ||\mathbf{P}_k\mathbf{m}||^2$$

where the measured samples of the mode are arranged in the column vector $\mathbf{m}$.

Once the wave number is known, the coefficients w_{nm} are then simply the coefficient of the projection of the mode in the basis of the plane waves considered.

It should be noted that the estimation of the wavenumber k_0 can be used to determine the dispersion curve of a plate, without need for complex experimental setup, as it is not affected by the boundary conditions of the plate. Reversibly, if one has some a priori information about the dispersion curve, this part of the algorithm is greatly simplified, as one only has to project the signal on the (here known) subspace E_k.

5. Experimental results

Figure 3 shows the experimental setup used to deploy the proposed IR interpolation method. Three plates are used : a rectangular plate of dimension 170mm × 190mm, free on three edges and clamped on a short edge, a plate of arbitrary shape with free edges, and a circular glass mirror with one segment cut off (radius $R = 210$ mm, thickness $h = 3$ mm, radius of cutting $R_i = 150$

mm), a shape that is well-known for exhibiting a chaotic-like behaviour, with free edges. The plates are isotropic and homogeneous. A circular piezoelectric transducer (PZT) is rigidly coupled to the plates. The PZT is driven by an audio amplifier in the frequency band 500 Hz - 22 kHz using a chirp excitation signal. Flexural waves are detected using a laser vibrometer. To determine the frequency response, every signal from the vibrometer is deconvolved by the excitation signal.

5.1. Modal decomposition of impulse responses

In practical implementations, the full SOMP algorithm is run only on a subset of 16 impulse responses, randomly chosen. Then, the dictionary (set of damped sinusoids) found by the algorithm is used to decompose the other responses. Analyzing only a subset of the signals keeps the computational and memory needs reasonable, while still having good accuracy. The damped sinusoids are chosen out of a set of sinusoids with more than 3.10^5 frequencies and 32 damping coefficients.

Figure 4 shows the residual energy at each step, compared to the residual energy of the best approximation using a fixed number of basis vector of the (undamped) Discrete Fourier Transform (DFT), for 16 channels of the rectangular plate. The sharp decrease of the residual for the damped sinusoids dictionary indicates that this is an efficient representation, whereas the Fourier transform is less compact : half of the energy is captured by 5 damped sinusoids, while this requires 608 DFT coefficients.

5.2. Mode interpolation

Rectangular plate In this section we compare the different methods for the reconstruction of a mode of the rectangular plate, at frequency 19 229 Hz. The sampling pattern for the Fourier interpolation is a regular sampling pattern, with 117 samples on a 13×9 grid, with a 15mm sampling step. The sampling pattern for the proposed scheme is 117 randomly placed sampling points. With this irregular sampling pattern, figure 5 shows the squared norm of the mode

projection on different subspaces E_k, normalized by the total energy of the mode. A peak is visible at $k = 154\text{m}^{-1}$ (peak value very close to 1): this value of k is the estimate of the wavenumber for this mode.

Reconstructions of the mode using Fourier interpolation and the proposed algorithm are shown on Figure 6, and compared to a reference measurement on a full 39×27 grid. To verify if the exponential plane waves are useful, results are also displayed using propagative plane waves only (Figure 6 d).

Since he 13×9 sampling grid verifies the Nyquist criterion, Fourier interpolation manages to interpolate correctly the mode in the interior domain of the plate, but fails at the border. The proposed algorithm, with or without exponential plane waves, yields correct reconstruction of the mode even at the borders.

Reconstruction of the interpolated impulse responses $\tilde{w}$ is achieved using coefficients $\tilde{w}^-_{nm}$ and $\tilde{w}^+_{nm}$ found by interpolating the modes, and the atoms c_n identified by SOMP:

$$\tilde{w}(x,y,t) = \sum_{n=0}^{N} c_n(t) \left(\sum_{m=1}^{M} \tilde{w}^-_{nm} e^{i\vec{k}_{nm}\cdot\vec{x}} + \sum_{m=1}^{M} \tilde{w}^+_{nm} e^{\vec{k}_{nm}\cdot\vec{x}} \right)$$

Figure 7 shows the signal to error ratio of the reconstruction on the plate, for Fourier interpolation, proposed algorithm with and without exponential plane waves. Mean interpolation SNR is respectively -19 dB, -30 dB and -29 dB. A measured impulse response and its interpolation from the 117 random measurements are plotted on figure 8.

Plate of arbitrary shape

The second plate is shown Figure 9, its dimension are approximately 370mm×130mm, with free borders. It is sampled on a grid of step 5mm, with 1455 points. A subset of these samples, with step 15mm (165 points), is used with Fourier interpolation, and compared to the result of the proposed method, with 165 random points, with and without evanescent waves. The interpolation error for these three methods is shown figure 10. Mean interpolation SNR is respectively -19 dB, -24 dB and -24 dB.

Results with this plate show that the proposed method with a non-convex plate with arbitrary boundaries.

Chaotic shaped plate Further results on the chaotic shaped plate show that the proposed method offers additional flexibility in the tradeoff between accuracy and number of measurements. Normal modes of the plate being approximated by few elementary functions (in our case plane waves), they are recoverable with few measurements. In this particular case, the modes are recovered with good accuracy using only 35% of the number of measurement needed to satisfy the Nyquist criterion. This achievement is an instance of the compressive sampling theory, where sampling efficiency is increased under sparsity conditions of the signal, at the cost of computational power. Note that in this part, measurements are made in an interior domain of the plate, and therefore exponential plane waves are discarded.

The impulse response are sampled on a 64×64 grid, with a 4mm sampling step. Three subsampling are used a regular grid of 256 samples with a 16mm step, and of 64 samples with a 16mm step, and a random pattern of 64 samples, which does not cover the lower left corner where the plate is excited. Reconstructions of the mode using the algorithm for the three samplings are shown on Figure 11. They are compared to Fourier interpolation for the two regular samplings. The fine sampling grid, with its sampling frequency above the Shannon-Nyquist rate, gives excellent reconstruction with the proposed method and Fourier interpolation. The irregular sampling gives similar results with only 64 samples, less than the half of the 169 required by the Shannon-Nyquist criterion for a uniform sampling. The coarse (Sub-Nyquist) regular grid gives an acceptable reconstruction of the mode with the proposed algorithm, while standard Fourier interpolation fails due to spectral aliasing. The success of the proposed algorithm in this case can be explained by the fact that, contrary to the Fourier interpolation where the reconstruction suffers from spectral aliasing, only the plane waves used for the decomposition and null at the sampling points are lost. The other plane waves can be distinguished from their aliases by their

wave number, which has to be equal to the one found by the optimization step of the algorithm.

The variation of the real part of the mode along the 17th column of the measurements is shown on Figure 12, with the results of the Fourier interpolation and the proposed method for the coarse sampling (samples indicated on the plot), and proposed method for irregular sampling (only one sample, not represented, lies on the column).

Figure 13 shows, for different number of measurements, the quality of the estimation of the 200 modes extracted by the SOMP algorithm. The Nyquist criterion, minimum number of measurements to avoid spectral aliasing, is here equal to

$$N_N = \left\lceil \frac{Lk}{\pi} \right\rceil^2$$

where $\lceil \cdot \rceil$ denotes the ceiling function (roundoff to smallest upper-bounding integer), and L is the width of the domain, while the number of measurements needed by our algorithm to recover correctly the modes is approximately

$$N_{pw} \simeq 5\frac{kL}{\pi}$$

While not the main goal of this study, this method provides an effective estimate of the dispersion curve of the plate. These estimations are plotted on Figure 14, for coarse regular sampling and irregular sampling. More than half of the modes lie in a range where the number of samples is too low to fulfill the Shannon-Nyquist criterion, without consequence on the reliability of the estimation. In low-frequency, plates have a dispersion relation of the form $\omega = ak^2$. The value of the parameter for the irregular sampling, obtained via a least-square fitting of the curve, is estimated at $a = 5.95$ m^2.s^{-1}. This value is very close to the result of a reference method [23], used on the same plate, which gave $a = 5.92$ m^2.s^{-1}.

Figure 15 shows the signal to error ratio of the reconstruction on the plate, for Fourier interpolation and proposed algorithm without exponential plane waves.

Mean interpolation SNR is respectively 0 dB and -25 dB. Figure 16 shows the first 200 samples of a measured impulse response (fine line) and its interpolation (dots) using 64 random measurements points on the plate. Note that the point of interest is located more than one wavelength of the mode of highest frequency away from the nearest measurement point, while the Nyquist criterion would imply that this distance never exceeds a half-wavelength.

As 2 seconds are needed to reliably measure an IR in this experimental setup, the full measurement of the IRs requires more than 2 hours, while undersampled measurements (2 minutes) and computation (10 minutes, on a standard computer) need 12 minutes, a tenfold improvement.

6. Conclusion

In this paper, an effective and practical method for the interpolation of homogeneous plate impulse responses is proposed. Based on a simple damping model and applied on plates with arbitrary shape and boundary conditions, this method allows the interpolation of IRs using a plane wave decomposition of the bending wave, in the whole audio range. While the main objective of the method is the identification of the plate modes, it also enables the determination of the dispersion curve of the plate. Thereby, the method needs no prior knowledge of the plate mechanical properties: as long as the part of the structure studied satisfies the Kirchhoff-Love model for a bending thin homogeneous isotropic plate, IR measurements are self-sufficient for interpolation, as demonstrated on a chaotic-shaped glass plate. Taking into account some prior physical knowledge to improve the efficiency of the acquisition process is an increasingly popular trend in the signal processing community, following the theory of compressive sampling. This comes at a significant increase in computational requirements, although these have become, in the last few years, achievable by standard PCs. However, when computational resources are scarce, when the physical assumptions are uncertain, or when acquisition time is unlimited, standard methods may be preferred.

Further extensions of the model and the algorithm will address the case of orthotropic plates, as well as theoretical bounds on the number of measurements needed for accurate interpolation.

7. Acknowledgements

GC acknowledges support from UPMC Univ Paris 06. GC and LD acknowledge partial support from Agence Nationale de la Recherche (ANR), project ECHANGE (ANR-08-EMER-006)

References

[1] D. M. Siringoringo, Y. Fujino, System identification of suspension bridge from ambient vibration response, Engineering Structures 30 (2008) 462 – 477.

[2] L. Wang, Z. Yang, T. Waters, Structural damage detection using cross correlation functions of vibration response, Journal of Sound and Vibration 329 (2010) 5070 – 5086.

[3] R. K. Ing, N. Quieffin, S. Catheline, M. Fink, In solid localization of finger impacts using acoustic time-reversal process, Applied Physics Letters 87 (2005) 204104.

[4] O. C. Zienkiewicz, The Finite Element Method in Engineering Science, McGraw-Hill, London, 1971.

[5] O. Cessenat, B. Despres, Application of an ultra weak variational formulation of elliptic pdes to the two-dimensional helmholtz problem, SIAM J. Numer. Anal. 35 (1998) 255–299.

[6] P. Rouch, P. Ladevèze, The variational theory of complex rays: a predictive tool for medium-frequency vibrations, Computer Methods in Applied Mechanics and Engineering 192 (2003) 3301 – 3315. Multiscale Computational Mechanics for Materials and Structures.

[7] S. W. Kang, S. Atluri, Free vibration analysis of arbitrarily shaped polygonal plates with simply supported edges using a sub-domain method, Journal of Sound and Vibration 327 (2009) 271 – 284.

[8] S. W. Kang, J. M. Lee, Free vibration analysis of arbitrarily shaped plates with clamped edges using wave-type functions, Journal of Sound and Vibration 242 (2001) 9 – 26.

[9] E. J. Candès, M. B. Wakin, An introduction to compressive sampling, IEEE Signal Processing Magazine (2008) 21–30.

[10] H. Rauhut, Random sampling of sparse trigonometric polynomials, Appl. Comput. Harmon. Anal. 22 (2007) 16–42.

[11] S. Kunis, H. Rauhut, Random sampling of sparse trigonometric polynomials II - orthogonal matching pursuit versus basis pursuit, Found. Comput. Math. 8 (2008) 737–763.

[12] Y. Haneda, Y. Kaneda, N. Kitawaki, Common-acoustical-pole and residue model and its application to spatial interpolation and extrapolation of a room transfer function, IEEE Trans. Speech Audio Processing 7 (1999) 709–717.

[13] A. Leissa, Vibration of Plates, NASA, Washington, 1969. Page 1.

[14] A. Moiola, R. Hiptmair, I. Perugia, Approximation by Plane Waves, Research Report 2009-27, Eidgenössische Technische Hochschule Zürich, 2009.

[15] E. Perrey-Debain, Plane wave decomposition in the unit disc: Convergence estimates and computational aspects, Journal of Computational and Applied Mathematics 193 (2006) 140 – 156.

[16] J. T. Chen, I. L. Chen, K. H. Chen, Y. T. Lee, Y. T. Yeh, A meshless method for free vibration analysis of circular and rectangular clamped plates using radial basis function, Eng. Anal. Boundary Elem. 28 (2004) 535–545.

[17] S. Reutskiy, The method of fundamental solutions for problems of free vibrations of plates, Engineering Analysis with Boundary Elements 31 (2007) 10 – 21.

[18] C. J. S. Alves, P. R. S. Antunes, The method of fundamental solutions applied to the calculation of eigensolutions for 2d plates, International Journal for Numerical Methods in Engineering 77 (2009) 177–194.

[19] R. Gribonval, H. Rauhut, K. Schnass, P. Vandergheynst, Atoms of all channels, unite! average case analysis of multi-channel sparse recovery using greedy algorithms, Journal of Fourier Analysis and Applications 14 (2008) 655–687.

[20] M. M. Goodwin, M. Vetterli, Matching pursuit and atomic signal models based on recursive filter banks, IEEE Transactions on Signal Processing 47 (1999) 1890–1902.

[21] S. Mallat, Z. Zhang, Matching pursuits with time-frequency dictionaries, Signal Processing, IEEE Transactions on 41 (1993) 3397–3415.

[22] A.-J. van der Veen, E. F. Deprettere, A. L. Swindlehurst, E. F. Deprettere, Subspace based signal analysis using singular value decomposition, Proceedings of the IEEE 81 (1993) 1277–1308.

[23] N. Etaix, A. Leblanc, M. Fink, R. K. Ing, Thickness or phase velocity measurements using the green function comparison method, IEEE Trans. Ultrason. Ferroelectr. Freq. Control 57 (2010) 1804–1812.

List of Figures

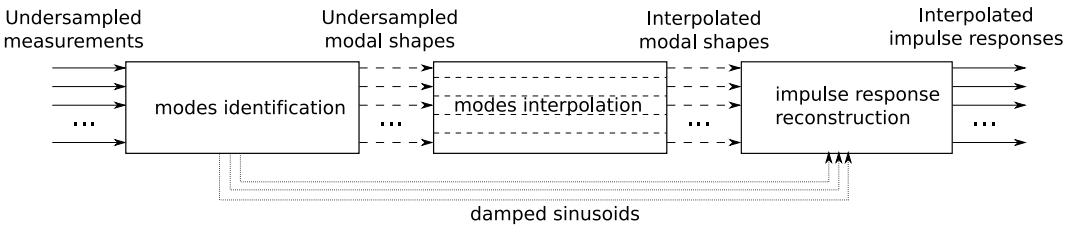

Figure 1: Diagram of the interpolation method

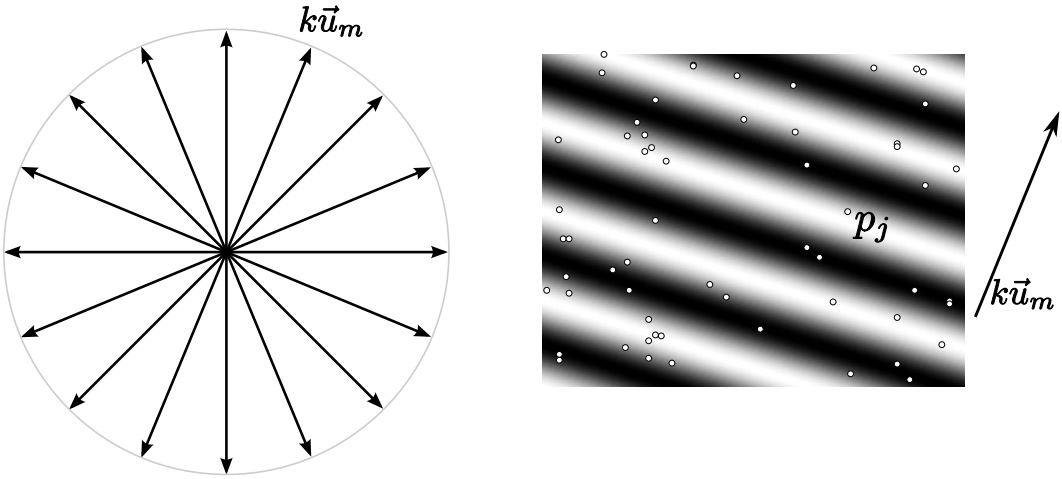

Figure 2: Discretization of the wave vectors for a given wave number k, and a plane wave sampled at the points p_j

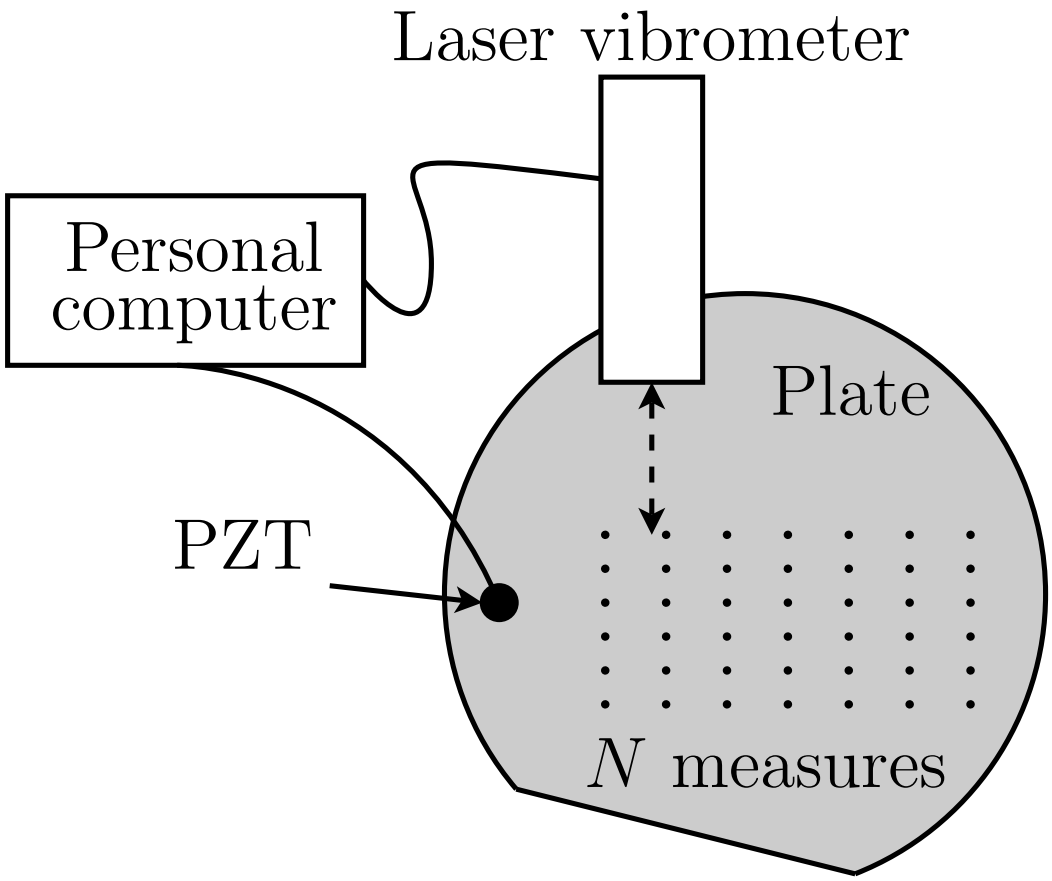

Figure 3: Experimental setup

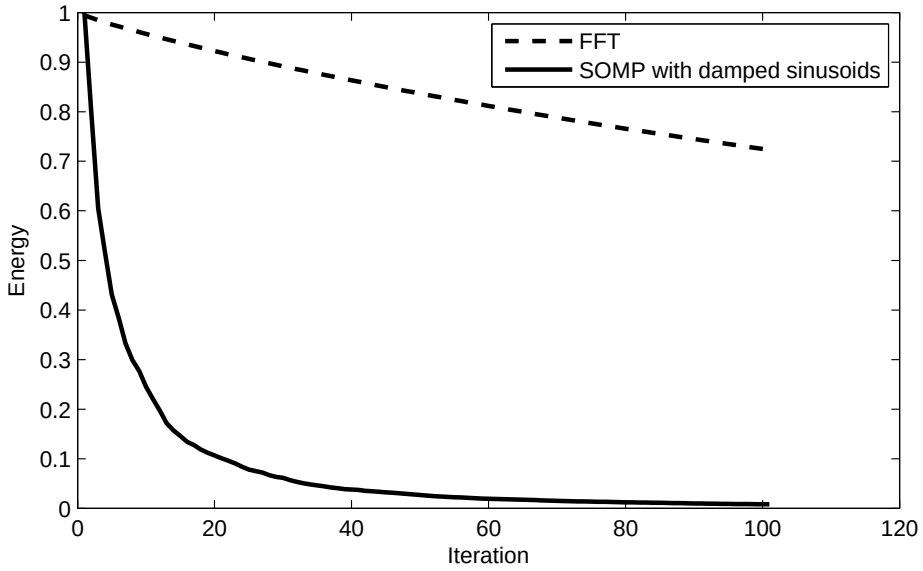

Figure 4: Approximation residual normalized by the total energy, for the SOMP algorithm and the best approximation with a fixed number of FFT coefficients and 16 channels

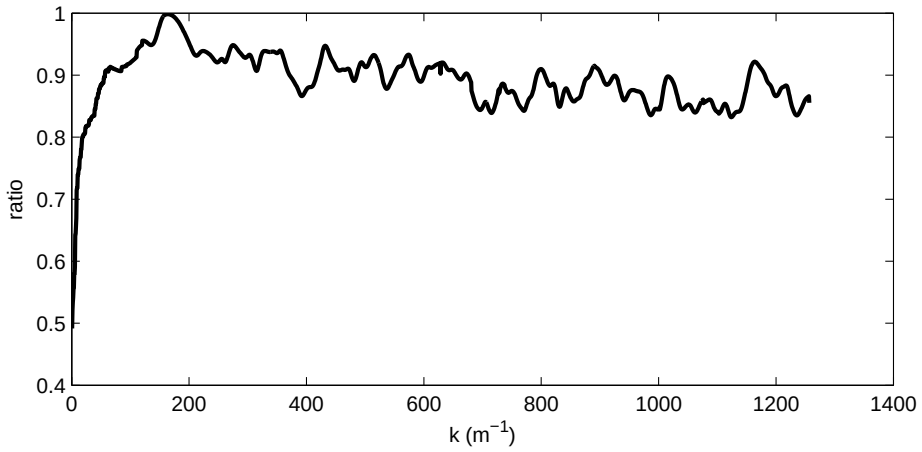

Figure 5: Ratio of energy lying in the subspace E_k spanned by 96 plane waves of wavenumber k, normalized by total energy. $f = 19229$ Hz.

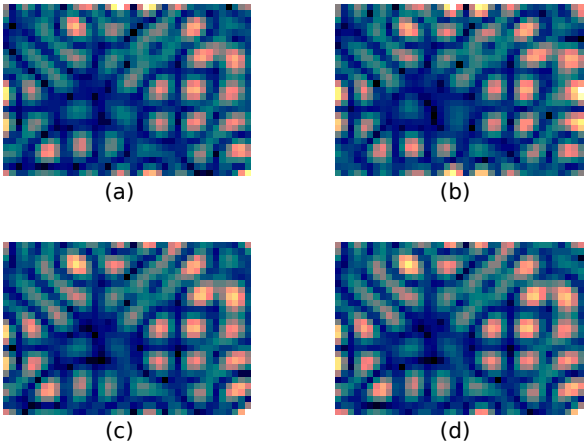

Figure 6: Vibration mode at $f = 19229$ Hz reconstructed by different interpolation methods. (a) reference measurement with a full 39×27 sampling (b) reconstruction with Fourier interpolation (c) reconstruction with the proposed method (d) reconstruction with the proposed method with propagative plane waves only.

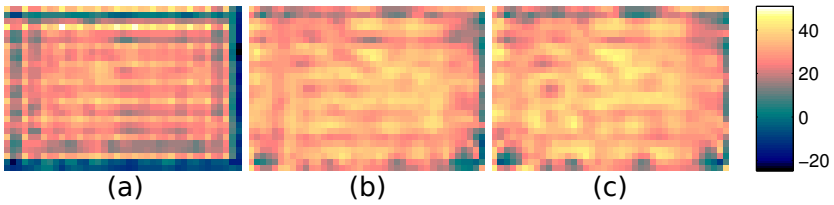

Figure 7: SNR of the Fourier interpolation (a) and the interpolation given by the proposed algorithm for the rectangular plate, with evanescent waves (b), and without (c)

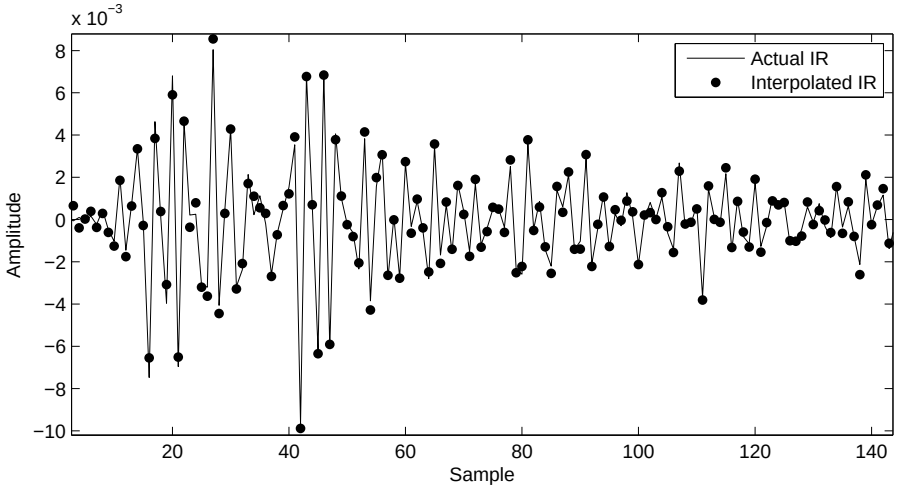

Figure 8: Measured impulse response on the rectangular plate, and its interpolation using 117 measurements

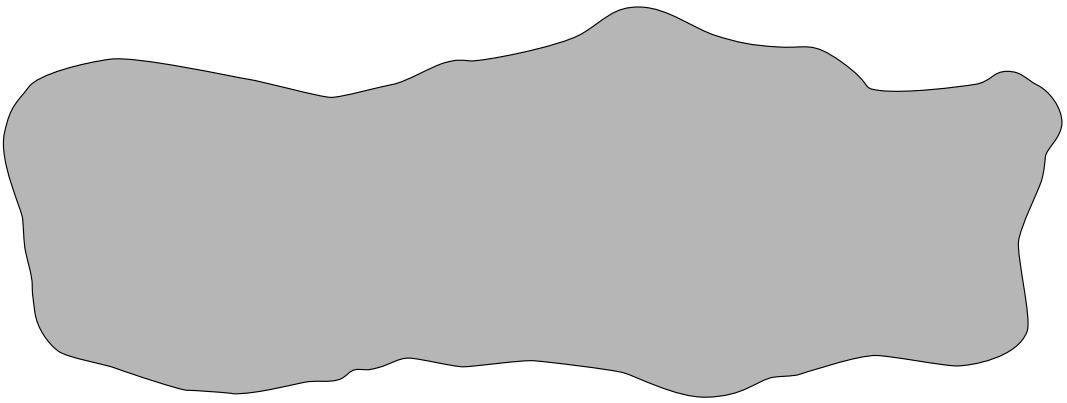

Figure 9: Plate of arbitrary shape

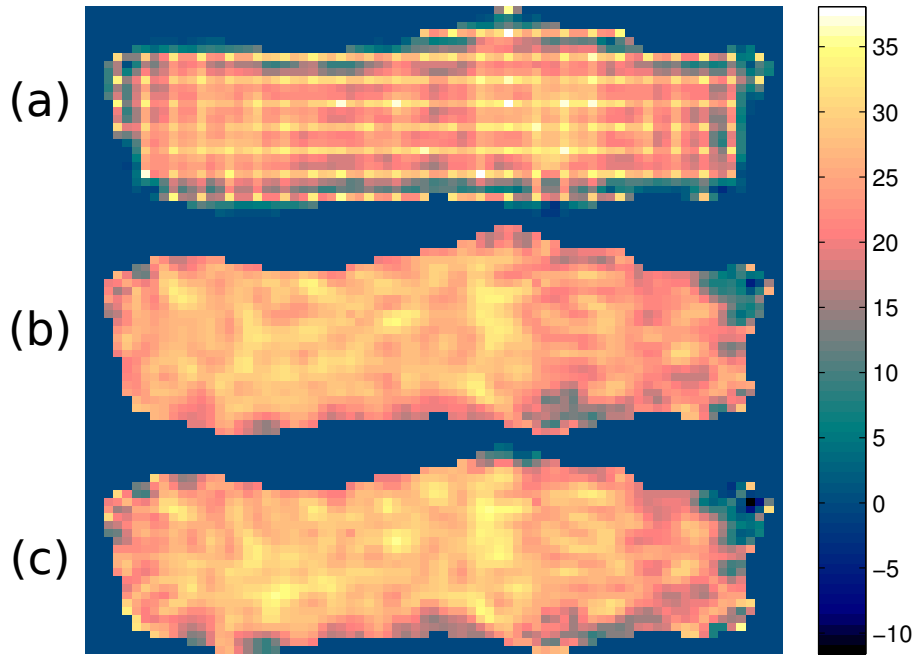

Figure 10: SNR of the Fourier interpolation (a) and the interpolation given by the proposed algorithm for the plate with arbitrary shape, with evanescent waves (b), and without (c)

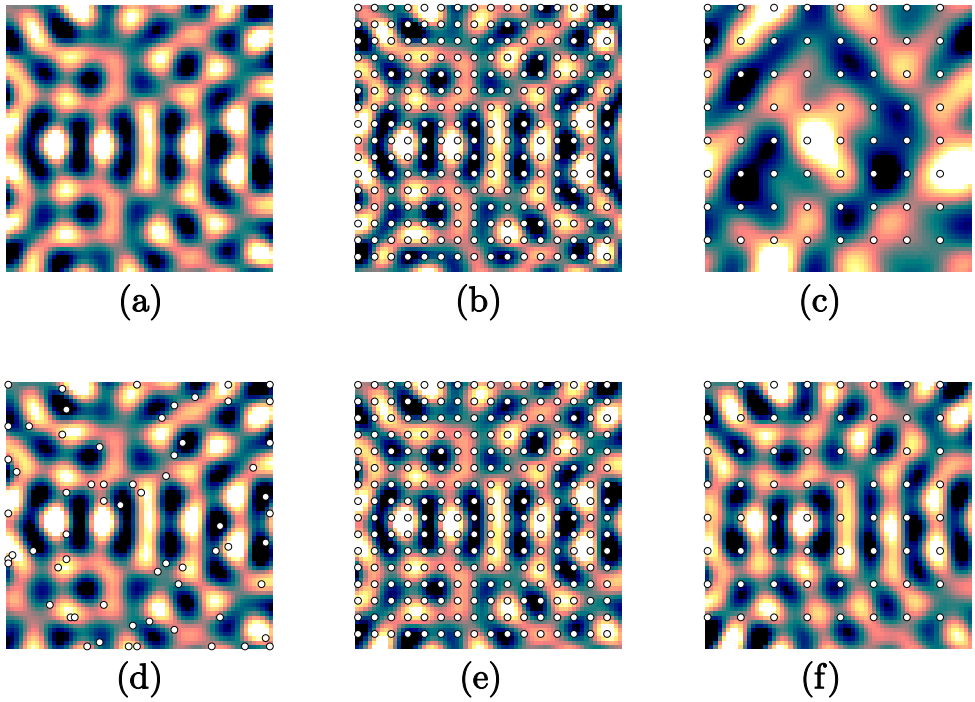

Figure 11: Vibration mode at $f = 20452$ Hz reconstructed by different sampling patterns, with sampling points marked as white dots. (a) reference measurement with a full 64×64 sampling (b) reconstruction with the fine regular grid (note that the Nyquist condition is still verified) and (c) reconstruction with the coarse (sub-Nyquist) regular grid with Fourier interpolation (d) reconstruction with the random grid (e) the fine grid and (f) the coarse grid with the proposed method.

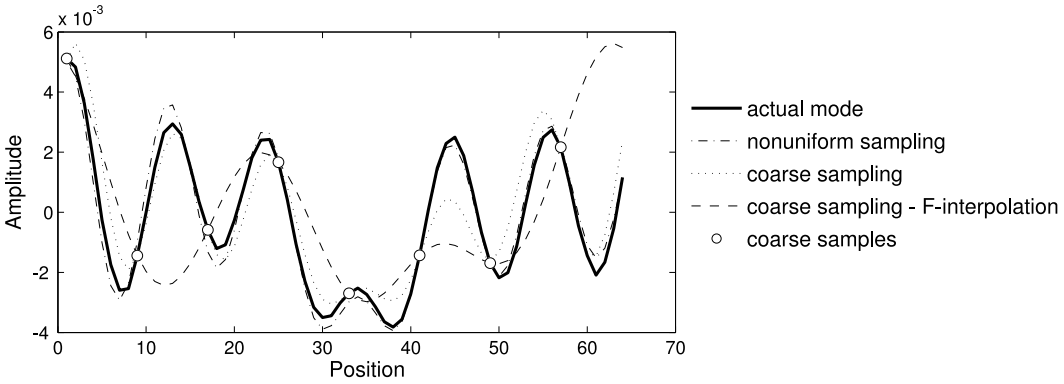

Figure 12: Plot of the real part of the $f = 20452$ Hz mode along a line. Ground truth, Fourier interpolation with coarse samples, proposed interpolation with coarse regular samples and irregular samples. Coarse regular samples are indicated with white circles. Only one sample of the irregular grid lies on the line. The imaginary part shows similar behavior.

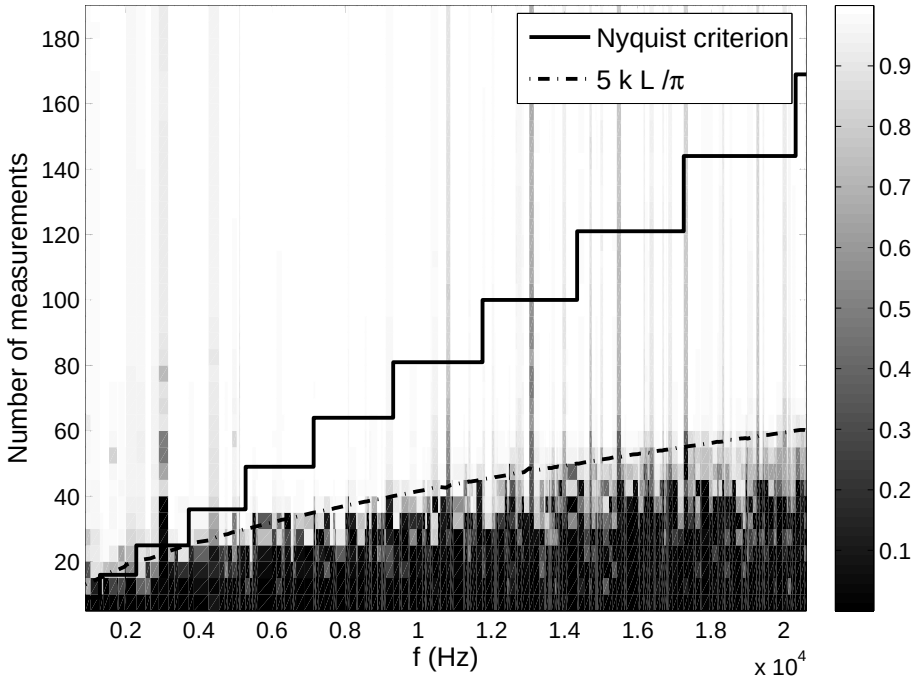

Figure 13: Correlation between the estimated modes and ground-truth measurements for the 200 modes identified, and number of measurements ranging from 5 to 185. The Nyquist criterion and the limit between correct and failed estimations for our algorithm are indicated.

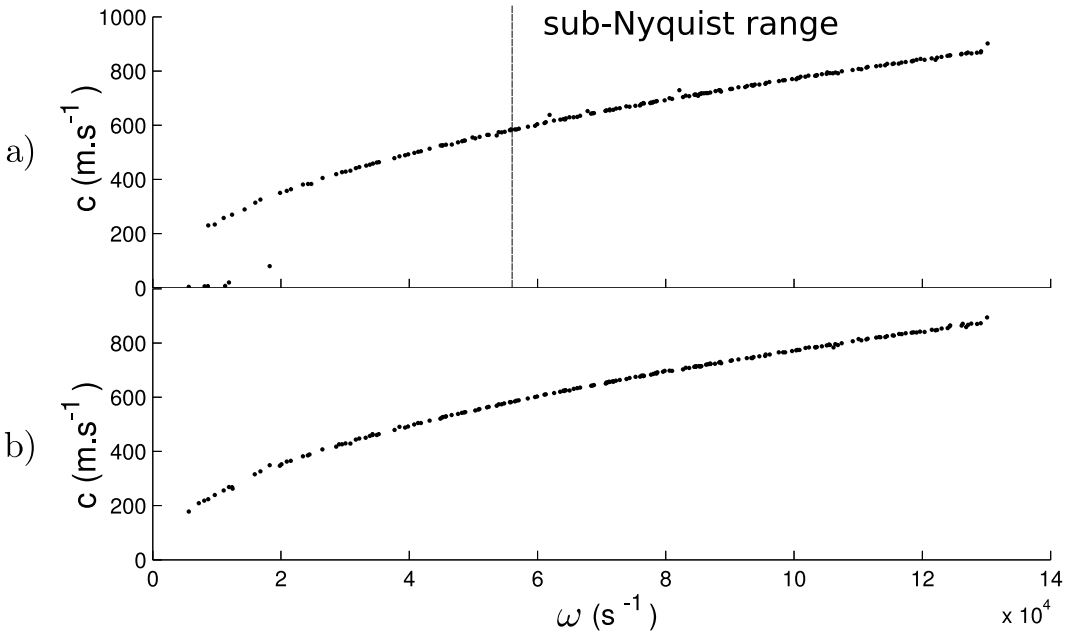

Figure 14: Estimated dispersion curves (a) with the coarse regular grid (64 samples) and (b) with the random grid (64 samples)

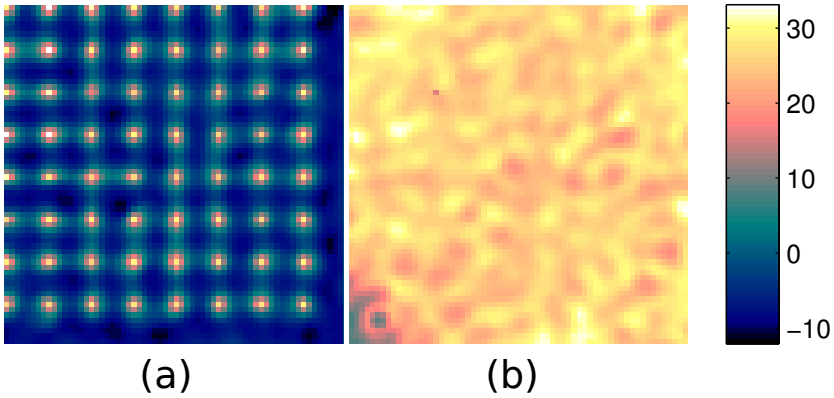

Figure 15: SNR of the Fourier interpolation (a) and the interpolation given by the proposed algorithm (b) for an interior square domain of the circular plate

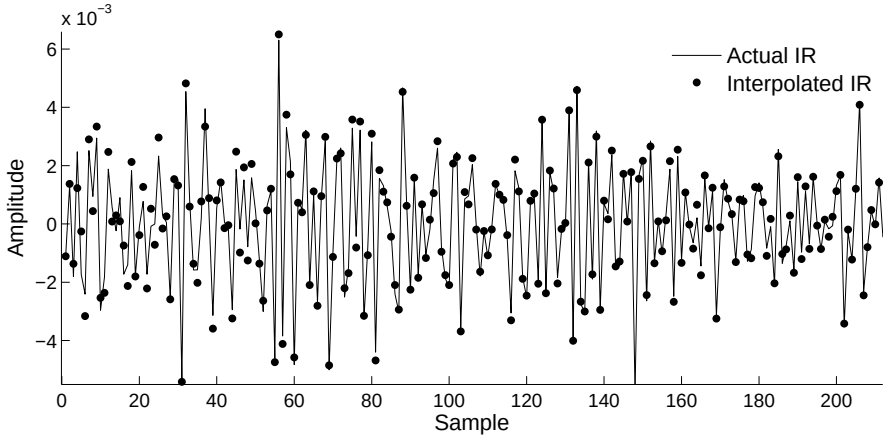

Figure 16: Plot of a measured impulse response, and its estimation using 64 random measurements.